IL-20 is an arteriogenic cytokine that remodels collateral networks and improves functions of ischemic hind limbs

Katerina Tritsaris*, Maja Myren*, Sisse B. Ditlev*, Martin V. Hübschmann*, Ida van der Blom†, Anker Jon Hansen†, Uffe B. Olsen†, Renhai Cao‡, Junhang Zhang§, Tanghong Jia¶, Eric Wahlberg§, Steen Dissing*, and Yihai Cao‡‖

*Department of Cellular and Molecular Medicine, Panum Institute, University of Copenhagen, Copenhagen 2200N, Denmark; †Novo Nordisk A/S, 2760 Måløv, Denmark; ‡Department of Microbiology, Tumor, and Cell Biology and §Division of Vascular Surgery, Department of Molecular Medicine and Surgery, Karolinska Institutet, 171 77 Stockholm, Sweden; and ¶Clinical Medical College, Shandong University, Jinan, Shandong 250012, China

Communicated by Judah Folkman, Harvard Medical School, Boston, MA, August 3, 2007 (received for review April 15, 2007)

Successful therapeutic angiogenesis for the treatment of ischemic disorders relies on selection of optimal proangiogenic or arteriogenic agents that are able to promote establishment of functional collateral networks. Here, we show that IL-20, a pleiotropic inflammatory cytokine, displays an imperative effect on vascular remodeling. Stimulation of both large and microvascular endothelial cells with IL-20 leads to activation of receptor-dependent multiple intracellular signaling components, including increased phosphorylation levels of JAK2/STAT5, Erk1/2, and Akt; activation of small GTP-binding proteins Rac and Rho; and intracellular release of calcium. Surprisingly, IL-20 significantly promotes endothelial cell tube formation without affecting their proliferation and motility. These findings suggest that the vascular function of IL-20 involves endothelial cell organization, vessel maturation, and remodeling. Consistent with this notion, delivery of IL-20 to the ischemic muscle tissue significantly improves arteriogenesis and blood perfusion in a rat hind-limb model. Our findings provide mechanistic insights on vascular functions of IL-20 and define therapeutic implication of this cytokine for the treatment of ischemic disorders.

arteriogenesis | collateral growth | therapeutical angiogenesis | ischemia

Despite available proangiogenic factors, therapeutic angiogenesis for the treatment of ischemic diseases, including coronary arterial diseases and various peripheral arterial diseases, has failed to conclusively show clinical benefits (1). Among several plausible reasons for clinical failures, the choice of an optimal angiogenic agent and understanding the underlying mechanisms of establishment of functional collateral networks in ischemic tissues are crucial issues for future development of successful therapeutic strategies. The establishment of collateral networks might involve both processes of collateral growth and remodelling of preexisting collaterals (2, 3). Several inflammatory cytokines have been shown to act as arteriogenic factors that might be useful for the treatment of ischemic disorders (4). The pleiotropic inflammatory cytokine IL-20 belongs to the IL-10 family, including IL-10, IL-19, IL-22, IL-24, and IL-26. IL-20 is expressed in monocytes, epithelial, and endothelial cells (5) and exerts its biological functions on multiple cells through activation of IL-20R1/IL-20R2 or IL-22R1/IL-20R2 complexes (6). For example, the interaction of IL-20 with IL-20R1 and IL-20R2 results in hyperproliferation of keratinocytes and development of pathological skin disorders such as psoriasis (6). IL-20-induced accumulation of inflammatory cells in various tissues could also be involved in the onset and progression of other inflammatory diseases, such as rheumatic arthritis and atherosclerosis (7). Interestingly, psoriasis, rheumatic arthritis, and atherosclerosis are all angiogenesis-dependent disorders, suggesting the possible role of IL-20 in regulation of angiogenesis.

Recently, IL-20 was reported to stimulate endothelial cell proliferation and migration and suggested to promote tumor angiogenesis (8). In this article, we show that IL-20 potently induces endothelial cell tube formation without affecting their proliferation and migration, suggesting that this cytokine plays an important role in vessel remodelling. In a rat ischemic hind-limb model, delivery of IL-20 significantly promotes reestablishment of collateral networks and blood perfusion in the ischemic skeletal muscle tissue. These findings demonstrate that IL-20 could be used as an arteriogenic cytokine for the treatment of ischemic diseases.

Results

***In Vivo* Angiogenic Activity.** To study the *in vivo* angiogenic activity, IL-20 was examined in the mouse corneal and matrigel angiogenesis models. At day 5 after implantation, IL-20 induced corneal neovascularization in mice, although its angiogenic activity was less potent than those stimulated by VEGF-A or FGF-2 (Fig. 1 *A–D*). The IL-20-induced corneal blood vessels appeared as well organized vasculatures, which consisted of individual microvessels separated from each other (Fig. 1*B*). Similar well defined vessels also existed in the FGF-2-induced vasculature (Fig. 1*D*). In contrast, VEGF-A-stimulated vessels appeared as a primitive vascular network composing of capillaries fused into vascular plexuses (Fig. 1*C*). Quantification analysis showed that IL-20 significantly induced corneal neovascularization as compared with slow-release polymer alone (Fig. 1 *E* and *F*).

IL-20 Promoted Tube Formation of ECs Isolated from Large and Small Vessels. To study direct effects of IL-20 on ECs, cell proliferation, migration, and tube formation assays were performed. IL-20 stimulated neither proliferation (0.5–5 nM) of porcine aorta endothelial (PAE) and human dermal microvessel endothelial (HDME) cells nor migration (0.5–100 nM) of PAE and human umbilical vein endothelial cells [supporting information (SI) Fig. 5]. However, when PAE cells were stimulated by IL-20, cell shape changes occurred, resulting in elongated cell structures. Interestingly, IL-20 was able to induce PAE (Fig. 2 *G–I*) and bovine capillary endothelial (BCE) (Fig. 2 *J–L*) cell sprouts that appeared as cord-like structures in a collagen spheroid assay. FGF-2 displayed a more potent effect than IL-20 in this system (Fig. 2*I*). Similarly, IL-20 potently stimulated tube formation of HDME cells in a matrigel assay, compared with buffer alone (Fig. 2 *M* and *N*). VEGF-A as

Author contributions: K.T., M.M., I.v.d.B., A.J.H., U.B.O., R.C., J.Z., E.W., S.D., and Y.C. designed research; K.T., S.B.D., M.V.H., I.v.d.B., U.B.O., R.C., J.Z., and S.D. performed research; K.T., M.M., S.B.D., M.V.H., A.J.H., R.C., J.Z., E.W., S.D., and Y.C. analyzed data; and K.T., A.J.H., S.D., and Y.C. wrote the paper.

The authors declare no conflict of interest.

Freely available online through the PNAS open access option.

Abbreviations: BCE, bovine capillary endothelial; $[Ca^{2+}]_i$, intracellular Ca^{2+} concentration; eNOS, endothelial nitric oxide synthase; HDME, human dermal microvessel endothelial; PAE, porcine aorta endothelial; VEGFR, vascular endothelial growth factor receptor.

‖To whom correspondence should be addressed. E-mail: yihai.cao@ki.se.

This article contains supporting information online at www.pnas.org/cgi/content/full/0707302104/DC1.

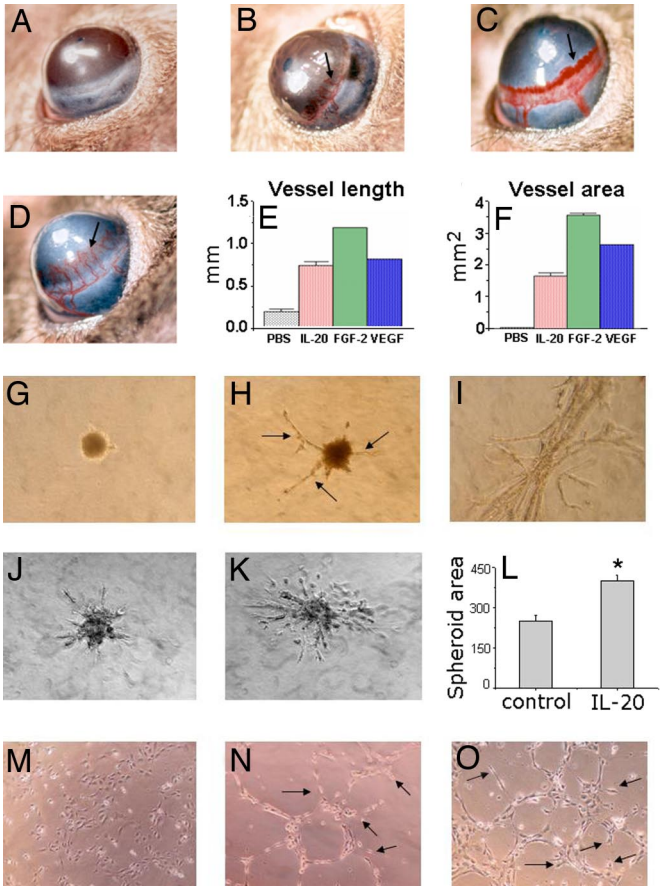

Fig. 1. Stimulation of corneal angiogenesis, endothelial cell sprouting, and tube formation. (*A–D*) A micropellet containing PBS (*A*), IL-20 (*B*), VEGF-A (*C*), or FGF-2 (*D*) with a slow-release polymer was implanted into the mouse cornea. At day 5 after implantation, corneal neovascularization (as indicated by arrows) was measured and photographed. (*E* and *F*) Corneal neovascularization was quantified as vessel length (*E*) and vascular area (*F*) as described in ref. 3. (*G–L*) Spheroids containing 750 PAE (*G–I*) or BCE (*J–L*) cells were embedded in collagen gels together with buffer (*G* and *J*), 5 nM IL-20 (*H* and *K*), or 30 ng/ml FGF-2 (*I*). Spheroid sprouting was imaged 2 (BCE) or 5 (PAE) days after incubation. (*L*) Sprouts from BCE control spheroids ($n = 8$) and IL-20-stimulated spheroids ($n = 10$) were quantified as described in *Materials and Methods*. (*M–O*) HDME cells were plated on a thin layer of matrigel and allowed to settle for 1 h before stimulation with saline (*M*), 5 nM IL-20 (*N*), or 20 ng/ml VEGF (*O*). Sprouting and branching are indicated by arrows.

a positive control was also able to induce tube formation of these endothelial cells (Fig. 2*O*). These findings demonstrate that IL-20 displays a selective effect on endothelial cell organization rather than stimulation of cell proliferation and migration.

Expression of IL-20 Receptors in Arterial and Capillary ECs. The transcripts of all three forms of IL-20 receptors, IL-20R1, IL-20R2, and IL-22R1, were detected in PAE and HDME cells by RT-PCR (Fig. 2*A*). Presence of IL-22R1 in both PAE and HDME cells was confirmed by real-time PCR (data not shown). Consistent with the patterns of mRNA expression, proteins of all three receptors were detectable in PAE cells by immunoblotting (Fig. 2*B*). These findings show that ECs of both arterial and capillary origin express IL-20 receptors.

Activation of Intracellular Signaling Components in ECs. Expression of IL-20 receptors in ECs suggested a direct effect of this cytokine on ECs. We studied signaling pathways involved in IL-20-induced EC activity and found that incubation of PAE cells with 5 nM IL-20 resulted in an initial dephosphorylation of Akt (Ser-473) and Erk1/2 kinases (Tyr-204) within the first 10 min after stimulation followed by a phosphorylation process causing elevated levels of phosphorylated Akt and Erk1/2 (Fig. 2 *C* and *D*). After 20 min of stimulation, levels of the phosphorylated Akt and Erks were significantly higher than those of nontreated PAE cells. Phosphorylated Stat5 (Tyr-694) and Jak2 (Tyr-1007/1008) were also detected in PAE cells in response to IL-20 resulting in maximum phosphorylation in <10 min. (Fig. 2 *E* and *F*). Additionally, exposure of either PAE, HDME, or BCE cells to IL-20 resulted in a rapid increase of intracellular Ca^{2+} concentration ($[Ca^{2+}]_i$) (Fig. 2 *G–J*). The elevated levels of $[Ca^{2+}]_i$ induced by IL-20 occurred immediately after IL-20 addition in some cells, whereas other cells displayed a delayed response of $[Ca^{2+}]_i$ release (Fig. 2 *G–I*). In contrast, VEGF-A only induced a delayed response of at least 30 sec (Fig. 2*J*). When cells were stimulated by sphingosine 1-phosphate that activates G protein-coupled receptors, release of $[Ca^{2+}]_i$ occurred at once and had a relatively short duration of ≈100 sec (Fig. 2*I*). The fluctuations in $[Ca^{2+}]_i$ induced by IL-20, VEGF-A, and sphingosine 1-phosphate were caused by release of Ca^{2+} from intracellular stores, because increases of $[Ca^{2+}]_i$ were also observed in Ca^{2+}-free media (data not shown) and were completely inhibited by U73122, an inhibitor of phospholipase C enzymes (Fig. 2 *K–L*).

Because Akt and increased $[Ca^{2+}]_i$ are strong regulators of endothelial nitric oxide synthase (eNOS) activity in endothelial cells, we investigated whether the observed Akt activation and the high levels of $[Ca^{2+}]_i$ resulted in NO synthesis. Measurements of NO synthesis showed that IL-20 increased intracellular levels of NO in PAE cells (Fig. 2 *M* and *N*). NO synthesis occurred in the perinuclear region and near the plasma membrane of IL-20 or VEGF-A-stimulated PAE, HDME, and BCE cells (Fig. 2 *M–O* and SI Fig. 6).

Sprouting and morphological changes, such as elongation followed by spreading, are considered prerequisites for formation of new capillary blood vessels (9). The morphology changes induced by IL-20 prompted us to investigate whether the small GTPases Rac and Rho were activated through GTP binding and to which extent actin polymerization processes were affected. Fig. 3 *A* and *B* shows that the activated form of Rho, Rho-GTP, was formed with maximal GTP binding observed after 10 min. This was consistent with the observed actin polymerization processes visualized in Fig. 3 *C–H* in PAE and HDME cells. Furthermore, Rac-GTP was remarkably increased (Fig. 3 *A* and *B*) with a biphasic activation curve. A rapid increase was seen within the first 5 min, followed by a sustained increase in Rac-GTP after 20 min. Thus, actin fibers became more abundant and underwent reorganization in the IL-20-stimulated PAE and HDME cells (Fig. 3 *C–H*).

Stimulation of Collateral Growth and Improvement of Blood Perfusion. To study therapeutic implications of IL-20 for the treatment of ischemic disorders, we established a severe rat ischemic hind-limb model in which long lasting severe ischemia was produced in the left leg (10). Ischemia was created by a two-step surgical procedure. This ischemic model can be considered relevant for leg ischemia found in patients. To monitor the establishment of stable collateral vessels, we performed angiographic analysis at day 42 (relatively long term) after the second operation. Delivery of IL-20 protein to the ischemic muscle tissue demonstrated a significant effect of IL-20 on stimulation of collateral growth in the ischemic muscle tissues around the ligation site (Fig. 4*B*). Remarkably, the IL-20-induced collaterals had developed into well established arteries appearing as corkscrew-shaped vessels forming vascular networks around the ligation site. Although buffer-treated hind limbs also displayed a moderate reestablishment of collateral networks, this outcome was generally considered the natural response to the occlusion of the femoral artery (3). Quantification analysis showed that the number of IL-20-induced collaterals was significantly higher than the buffer-treated control group (Fig. 4*G*).

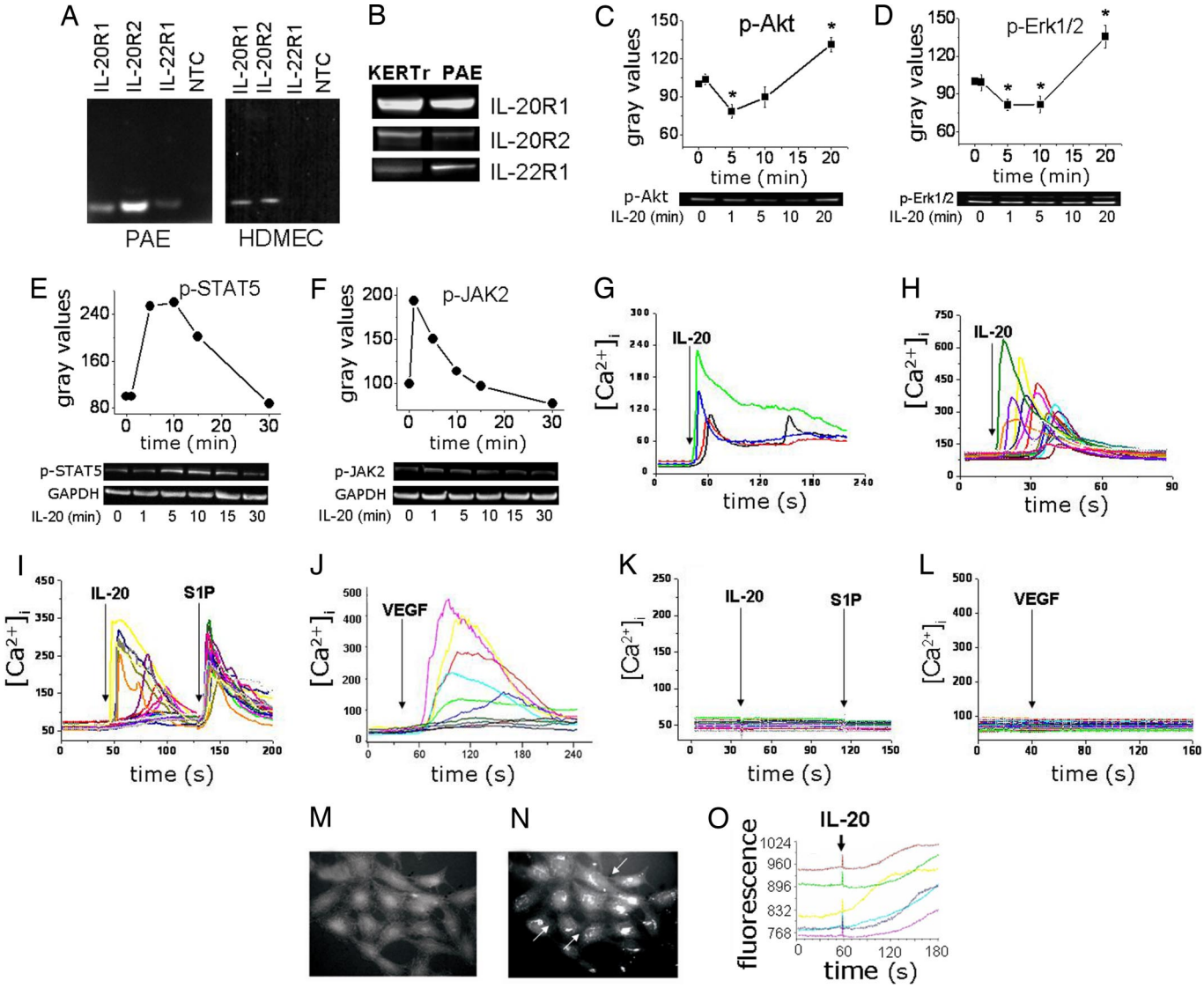

Fig. 2. Expression of IL-20 receptors and IL-20-induced intracellular signaling. (*A*) RT-PCR was performed by using total RNA isolated from PAE/VEGFR-2 and HDME cells, and the amplified fragments of IL-20R1, IL-20R2, and IL-22R1 were visualized on an agarose gel. (*B*) Cell lysates from PAE/KDR and human fetal skin keratinocyte (KERTr) cells were analyzed by immunoblotting, using IL-20R1, IL-20R2 or IL-22R1 primary antibodies. (*C–F*) PAE/VEGFR-2 cells were stimulated with 5 nM IL-20 at the indicated time points. The following Western blots were performed: *p*-Akt (*C*), *p*-Erk1/2 (*D*), *p*-STAT5 (*E*), or *p*-JAK2 (*F*). (*E* and *F*) Membranes were reprobed with an anti-GAPDH antibody. (*C* and *D*) Average of three experiments; error bars indicate standard deviation; *, $P < 0.05$. (*G–L*) HDME (*G*), BCE (*H*), PAE (*I* and *K*), and PAE/VEGFR-2 cells (*J* and *L*) were stimulated with IL-20, sphingosine 1-phosphate, and VEGF-A at the indicated time points. Each trace represents the recorded calcium level in a single cell. (*K* and *L*) Cells were preincubated with the PLC inhibitor U-73122 (5 μM). Each experiment represents more than five individual experiments. (*M* and *N*) Measurements of NO production before (*M*) and after (*N*) stimulation with 10 nM IL-20. (*O*) Traces were continuously recorded and represent NO production in single cells. The experiment is representative of five individual experiments.

To further validate the stimulatory effect of collateral growth by IL-20, we performed immunohistochemical analysis to quantify vascular smooth muscle cell-positive vessels in the treated ischemic muscle tissues. Vascular smooth muscle cell-positive vessels were present in the buffer-treated control samples; however, IL-20 significantly increased the number of arteries (Fig. 4 *F* and *I*). The increase of collateral numbers by IL-20 demonstrates this cytokine is able to induce new arterial vessel formation.

To study improvement of blood flow after IL-20 treatment, a laser Doppler analysis of paw skin perfusion was carried out at day 42 after the second ligation procedure. Consistent with angiographic findings, delivery of IL-20 significantly improved the paw blood perfusion in the ischemic hind limb (Fig. 4 *C*, *D*, and *H*). These results show that IL-20 induces the formation of functional collateral networks, which increase distal skin perfusion.

Discussion

In this article, we show that the inflammatory cytokine, IL-20, acts as an arteriogenic and vascular remodeling factor, which promotes the establishment of functional collateral networks in the ischemic skeletal muscles in rats and induces changes in cell morphology, tube formation, and sprouting of vessels *in vitro*. We found expression of IL-20R1, IL20R2, and IL-22R1 in PAE and HDME cells, and our data show that IL-20 activated a range of signaling processes that have been implicated in growth factor-activated angiogenic signaling pathways, including tyrosine phosphorylations of JAK2 and STAT5, activation of the serine and threonine kinases Akt and Erk1/2, and the small GTPases Rac and Rho. In addition, we report observed rapid Ca^{2+} and NO signaling. Stimulating PAE, HDME, and BCE cells with IL-20 resulted in a transient rise in $[Ca^{2+}]_i$ through release from intracellular stores. An increased level

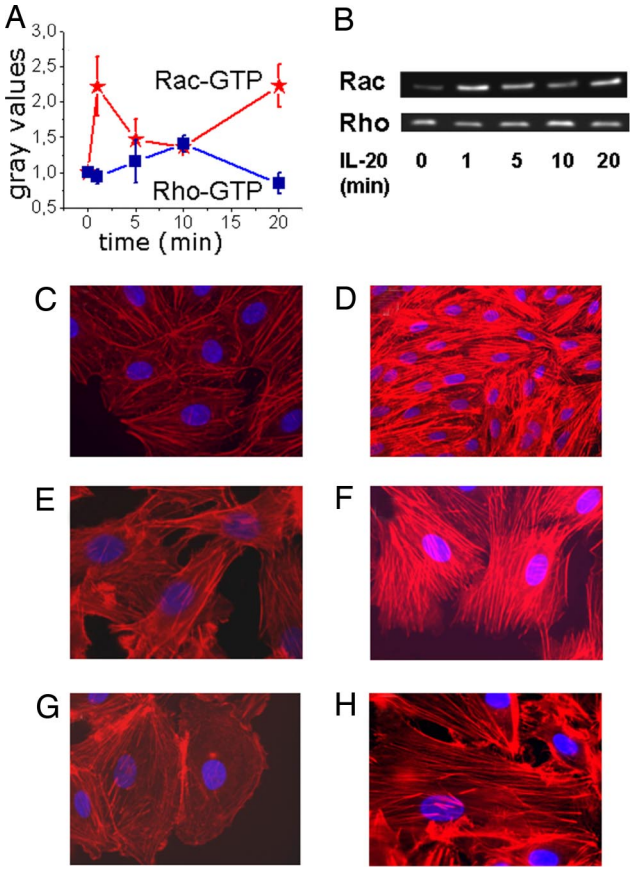

Fig. 3. IL-20 regulation of small GTPases and reorganization of the cytoskeleton. (*A* and *B*) Active Rac and Rho in PAE/VEGFR-2 cells after stimulation with 5 nM IL-20 were subsequently detected by pull-down assays and immunoblotting (*A*) and quantified densitometrically (*B*). Average of three experiments; error bars indicate standard deviation; *, $P < 0.05$. IL-20-induced stimulation of actin polymerization was visualized by staining fixed and permeabilized endothelial cells with phalloidin-rhodamin. (*C–F*) PAE cells were stimulated with saline (*C*) or 5 nM IL-20 (*D*) for 4 h or saline (*E*) or 5 nM IL-20 (*F*) for 24 h. (*G* and *H*) HDME cells were stimulated with saline (*G*) or 5 nM IL-20 (*H*) for 4 h. Representative of three individual experiments.

of $[Ca^{2+}]_i$ is a crucial step in a variety of cell activation processes involving enzymatic activations. One of those is the activation of eNOS leading to NO production and vasodilation. IL-20 induced pronounced and localized synthesis of NO near the perinuclear area and in the cell periphery. It has been shown that after stimulation, eNOS moves away from caveolae and distributes both at the plasma membrane and near Golgi, when stimulated with acetylcholine (11). We found NO synthesis mostly near the perinuclear region and near the plasma membrane area after stimulation with IL-20 (Fig. 2 *M–O*) and VEGF (see SI Fig. 6). Activation of Akt causes eNOS phosphorylation that together with an increase in $[Ca^{2+}]_i$ lead to NO synthesis. Our data are consistent with the rapid and strong increase in $[Ca^{2+}]_i$ after stimulation with IL-20 and the subsequent Akt phosphorylation being responsible for eNOS activation and NO synthesis. It is interesting to note that the NO synthesis, besides its role as a vasodilator, also facilitates most of the angiogenic processes (12). Several angiogenic factors stimulate NO synthesis, and the importance of this molecule is illustrated by eNOS knockout studies, revealing impaired angiogenesis in response to ischemia (12).

The IL-20-induced rise in $[Ca^{2+}]_i$ appears to be one of the essential signaling processes linking the IL-20 receptor to Rac activation and morphological changes (13). Interestingly, a recent study shows that VEGF-induced Rac activation in human umbilical vein endothelial cells is diminished by carbazole, the active antipsoriatic component of coal tar (14), implicating Rac as a signaling factor affecting angiogenesis during psoriasis development. Consistent with the very pronounced effects of IL-20 on the cytoskeleton in aortic and capillary endothelial cells, we also found that IL-20 increased Rho-GTP formation. Rho-GTP coordinates responses of endothelial cells to extracellular stimuli by regulating cell shape and polarity and cell-to-cell adhesion (see ref. 15 for a review). Thus, the activation by IL-20 of JAK2/STAT5, Akt, and Erk1/2 signaling (together with the rapid Ca^{2+} rise, NO synthesis, and activation of the small GTPases Rac and Rho) is consistent with IL-20 being a cytokine that can modulate angiogenic processes of which a number of biological effects are important, such as rearrangement of cytoskeleton, changes in morphology, and cell sprouting.

Establishment of functional collateral networks probably involves processes of both collateral growth and remodeling of preexisting collaterals. Some recent studies in rodent models support the latter mechanism (16). Unlike most of other known angiogenic factors and cytokines, IL-20 does not stimulate EC proliferation and migration of three independent cell lines. In contrast to our findings, a recent study showed that IL-20 played a direct role in stimulation of EC proliferation and migration (8). The discrepancy between that study and our present findings is unclear. Interestingly, in both *in vitro* and *in vivo* systems, IL-20 potently stimulates vessel tube formation. The origin of endothelial cells induced by IL-20 is unclear. It is possible that IL-20 is a chemoattractant for inflammatory cells, including neutrophils and monocytes/macrophages, which subsequently induce angiogenesis. Another possibility is that IL-20 might mobilize circulating precursor endothelial cells that participate in neovascularization. These possibilities warrant further investigation. If IL-20 had been assayed for its ability to stimulate EC growth, it would have had by definition been considered a nonangiogenic cytokine. The vascular remodeling activity of a growth factor or cytokine could, therefore, probably be assayed only in a 3D EC culture system and by appropriate *in vivo* angiogenesis models. It is interesting to note that IL-24, which acts on the same receptor complexes as IL-20, is anti-angiogenic. Like IL-20, it is without effect on EC proliferation *in vitro* but does inhibit tube formation (17). In addition, there are several examples of signaling systems including the notch pathway that control EC differentiation, vascular remodeling or arteriogenesis without significantly affecting EC growth (18). Genetic deletion of these genes in mice results in severe vascular patterning defects, leading to lethality of embryos during the early embryonic development (19). Thus, vascular remodeling (including EC differentiation, reorganization, trimming, and shaping of primitive vasculatures; recruitment of vascular smooth muscle cells or pericytes; and maintenance of the stable vasculature) is crucial for establishment of a functional arterial network.

Under a hypoxic environment, VEGF-A is usually up-regulated by activation of the HIF-1α pathway (20). However, VEGF-A alone as a relative specific endothelial growth factor might not be sufficient to induce arteriogenesis and VEGF-A-induced primitive vascular plexuses have to be remodeled (21). In agreement with this notion, delivery of VEGF-A alone to ischemic muscle tissues in patients did not produce conclusive beneficial effects (22). It is highly possible that IL-20 in the ischemic tissue could remodel VEGF-A-induced vessels. In addition to its direct effects on vascular remodeling, IL-20 might also regulate arteriogenesis via recruitment of inflammatory cells. In accordance with this notion, we found, using a Boyden chamber, that IL-20 is a chemotactic factor for monocytes (data not shown). Indeed, several inflammatory cytokines have been shown to stimulate arteriogenesis and the formation of collateral networks (4). IL-20 receptors are expressed on ECs, supporting its direct role in regulation of vessel formation. Interleukins, together with other immunoregulatory cytokines, might play an important role in switching on or off vessel growth

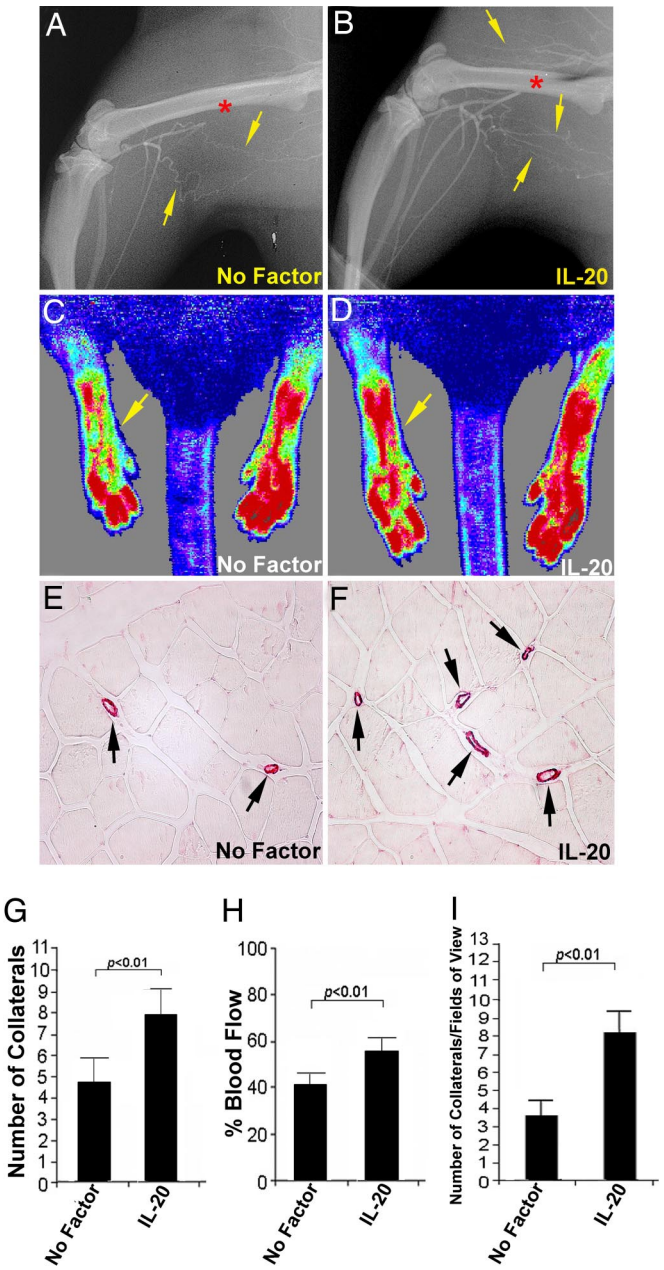

Fig. 4. Angiographic, immunohistochemical, and blood flow analyses of the rat ischemic hind limbs. Immediately after the second operation (ligation of the femoral artery), IL-20 or buffer alone in the same slow release polymer as described in the mouse micropocket neovascularization assay was implanted in the ligation site. Soluble IL-20 was also injected into the ligation site seven times every other day for 12 total days. (*A* and *B*) At day 42 after ligation of femoral artery, collateral growth was analyzed by using angiographic analysis and quantified by counting the number of collaterals in each leg. (*C* and *D*) Blood flow was measured by using a laser Doppler method on day 42. Arrows point to blood perfusion in the treated ischemic legs. (*E* and *F*) Immunohistochemical analysis of collateral growth, using an anti-a-SMA antibody. Arrows point to collaterals. (*G–I*) Numbers of collaterals detected by angiographic analysis (*G*) and immunohistochemistry (*I*) were presented as mean determinants (±SD); improvement of blood flow was presented as percentages to those of the healthy legs (*H*).

and in maintaining homeostasis of the vasculature. Our intriguing finding that IL-20 regulates vascular remodeling without affecting EC growth distinguishes this cytokine from others regarding the vascular function.

Functional improvement of ischemic tissues stipulates revascularization of arterial vascular networks that perfuse hyperoxygenated fresh blood to the ischemic region. Although molecular mechanisms of angiogenesis have been relatively well characterized, little is known about arteriogenesis, which is essential for therapeutic development. Successful arteriogenic therapy relies on the optimal choice of arteriogenic factors. Unfortunately, current therapeutic strategies lack rationales for selection of angiogenic or arteriogenic factors. IL-20 as a vascular remodeling factor that promotes the formation of functional collateral networks represents a new class of arteriogenic factor. Thus, this factor should hold a great promise for clinical development for the treatment of ischemic diseases.

Materials and Methods

Cells and Growth Factors. Vascular endothelial growth factor receptor (VEGFR)-2-expressing and nonexpressing PAE cells were established as reported in ref. 23 and grown in DMEM or Ham F-12 medium supplemented with 10% FCS. HDME cells (Promocell, Heidelberg, Germany) were grown in Endothelial Cell Growth Medium MV (Promocell), and human umbilical venous endothelial cells (human umbilical vein endothelial cells) were grown in endothelial basal medium-2 supplemented with growth factors (Cambrex, East Rutherford, NJ). BCE cells were grown in DMEM, including 1 ng/ml human basic FGF-2. Human fetal skin keratinocytes were obtained from American Type Culture Collection (Manassas, VA) and grown in a serum-free keratinocyte medium (GIBCO, Carlsbad, CA) supplemented with 0.05 mg/ml bovine pituitary extract and 35 ng/ml EGF. Recombinant IL-20 was obtained from Novo Nordisk and Biosource (Camarillo, CA), human VEGF was obtained from Sigma (St. Louis, MO), and FGF-2 was purchased from Sigma. Male 5- to 6-week-old C57BL/6 mice (MTC; Karolinska Institutet) were used for the corneal pocket assay and acclimated in groups of six or fewer per cage. For the rat hind-limb ischemia model, Sprague–Dawley male rats (B & K Universal, Sollentuna, Sweden) weighing 280 ± 20 g were used.

RT-PCR. Reverse transcription was performed by using total RNA from PAE/VEGFR-2 and HDME cells and Omniscript Reverse Transcriptase kit (Qiagen, Dorking, Surrey, U.K.). (See *SI Materials and Methods* for details.)

Western Blot. PAE/VEGFR-2 and human fetal skin keratinocyte cells were grown to 95% confluency in 60-mm dishes, washed with PBS, and incubated for 60 min in a serum-free medium (RPMI medium 1640) as described in ref. 24. (See *SI Materials and Methods* for details.)

Rac and Rho Activity Assays. Rac-GTP and Rho-GTP were measured by using Rac and Rho activation assay biochem kits (Cytoskeleton, Los Angeles, CA). (See *SI Materials and Methods* for details.)

Phalloidin Staining. HDME and PAE cells were grown on chambered cover-glass (Lab-Tek; Nalge Nunc International, Rochester, NY) to 90% confluency. Cells were serum- starved for 1 h (HDME cells) or 48 h (PAE) in RPMI medium 1640 before stimulation. Activation was stopped by removal of the media and cells were fixed, permeabilized, and stained with phalloidin-rhodamin according to the instructions provided by the supplier (Cytoskeleton).

Measurements of $[Ca^{2+}]_i$ and Nitric Oxide. The intracellular calcium concentration ($[Ca^{2+}]_i$) and NO formation were measured in HDME and PAE cells grown to 90% confluence in chambered cover-glasses (Lab-Tek; Nalge Nunc International) as described in ref. 25. (See *SI Materials and Methods* for details.)

Matrigel Tube Formation Assay. Growth factor-reduced matrigel matrix (BD Biosciences, Brøndby, Denmark) was added to 12-well culture plates according to the manufacturer's instruction, and the matrigel was allowed to polymerize for 30 min at 37°C. HDME cells (1×10^5) in growth medium were plated on the matrigel and stimulated after 1 h. After 4 h of incubation, tube formation was observed with a Lietz Labovert phase-contrast microscope ×150 magnification (Leica Microsystems, Herlev, Denmark), and images were acquired by using a digital camera (CoolPix 990; Nikon, Tokyo, Japan).

Spheroid *in Vitro* Angiogenesis Assay. An *in vitro* angiogenesis assay using PAE or BCE cell spheroids was performed principally as described in ref. 26. (See *SI Materials and Methods* for details.)

Mouse Corneal Micropocket Assay. The mouse corneal assay was performed as described in ref. 27. A micropellet (0.35 × 0.35 mm) of sucrose aluminum sulfate (Bukh Meditec, Copenhagen, Denmark) coated with hydron polymer-type National Ecological Observatory Network Coordinating Consortium containing 500 ng of IL-20, 160 ng of VEGF-A, or 80 ng of FGF-2 was surgically implanted into each micropocket in the mouse eyes (one eye per mouse). The corneal neovascularization was examined and quantified at day 5 after pellet implantation (n = 7–10 eyes per group). Vascularization areas were calculated by measuring vessel length and clock-hours (the circumferential area of neovascularization if the eye is considered as a clock).

Rat Ischemic Hind-Limb Model. The rat ischemic hind-limb model was carried out as described in ref. 10, using a two-stage procedure on the left hind limb. The right hind limb serves as a control. The operated animals were randomly divided into two groups (six rats per group) for treatment with IL-20 or PBS. During the second operation, 5 μg of IL-20 or PBS in sucrose sulfate/hydron slow-release polymers was implanted into intramuscular pockets near the ligation site. After completion of the operation, 50 μg of IL-20 in 400 μl of PBS or buffer alone were injected into three sites close to the femoral ligation site, and the treatment continued every other day for 12 days.

Laser Doppler Perfusion Imaging. The laser Doppler perfusion imager (MoorLDI-VR; Moor Instruments, Axminster, U.K.) was used to assess the limb perfusion. (See *SI Materials and Methods* for details.)

Angiography. At day 42 after the second operation, rats were anesthetized and a midline incision was performed to expose and place a ligature around the abdominal aorta. (See *SI Materials and Methods* for details.)

Immunohistochemistry. After killing the animals at day 42 after the second operation, muscle tissue samples from the ligated and treated areas of the ischemic and control hind limbs were dissected. Tissue samples were fixed with 3% paraformaldhyde overnight at 4°C, dehydrated and embedded in paraffin, and cut as 5-μm cross-sections. The muscle tissue was then stained with a monoclonal antibody against smooth muscle α-actin (Neomarkers, Fremont, CA). For further details, see *SI Materials and Methods*. Omission of the first antibody was used as a negative control. Analysis of tissue samples was conducted by using a Nikon Eclipse E800 epifluorescence microscope.

Collateral Analysis. Collateral numbers were measured from α-actin positively stained vessels, excluding the ones with a venous shape at ×10 magnification. A total number of collaterals were counted manually from 10 different fields selected from two different sections from each sample in a blinded fashion. The results were expressed as the number of collateral arteries per field of view.

Statistics. Data are presented as means ± SD or means ± SEM. Statistical evaluation of the results was made by two-tailed Student's t test and Mann–Whitney U test, using Statview and Microsoft (Redmond, WA) Excel softwares. Differences with $P < 0.05$ were considered significant.

We thank Pia Birn and Lene Grønne Pedersen for technical assistance. This study was supported by grants from the Vera Og Carl Jonah Michaelsens Legat (Charlottenlund, Denmark), the Swedish Heart and Lung Foundation (Stockholm, Sweden), the EU integrated project of VascuPlug Contract No. STRP 013811, the Söderberg Foundation (Stockholm, Sweden), and the Swedish Medical Research Council (Stockholm, Sweden).

1. Simons M, Ware JA (2003) *Nat Rev* 2:863–872.
2. Carmeliet P (2000) *Nat Med* 6:389–395.
3. Cao R, Brakenhielm E, Pawliuk R, Wariaro D, Post MJ, Wahlberg E, Leboulch P, Cao Y (2003) *Nat Med* 9:604–613.
4. Buschmann I, Heil M, Jost M, Schaper W (2003) *Microcirculation* 10:371–379.
5. Hsing CH, Ho CL, Chang LY, Lee YL, Chuang SS, Chang MS (2006) *Cytokine* 35:44–52.
6. Blumberg H, Conklin D, Xu WF, Grossmann A, Brender T, Carollo S, Eagan M, Foster D, Haldeman BA, Hammond A, *et al.* (2001) *Cell* 104:9–19.
7. Wei CC, Hsu YH, Li HH, Wang YC, Hsieh MY, Chen WY, Hsieng CH, Chang MS (2006) *J Biomed Sci* 13:601–612.
8. Hsieh MY, Chen WY, Jiang MJ, Cheng BC, Huang TY, Chang MS (2006) *Genes Immun* 7:234–742.
9. Folkman J (2003) *Curr Mol Med* 3:643–651.
10. Lundberg G, Luo F, Blegen H, Kalin B, Wahlberg E (2003) *Eur Surg Res* 35:430–438.
11. Sánchez FA, Savalia NB, Durán RG, Lal BK, Boric MP, Durán WN (2006) *Am J Physiol* 291:H1058–H1064.
12. Rudic RD, Shesely EG, Maeda N, Smithies O, Segal SS, Sessa WCJ (1998) *J Clin Invest* 101:731–736.
13. Price LS, Langeslag M, ten Looster JP, Hordijk PL, Jalink K, Collard JG (2003) *J Biol Chem* 278:39413–39421.
14. Arbiser JL, Govindarajan B, Battle TE, Lynch R, Frank DA, Ushio-Fukai M, Perry BN, Stern DF, Bowden GT, Liu A, *et al.* (2006) *J Invest Dermatol* 126:1396–1402.
15. Fryer BH, Field J (2005) *Cancer Lett* 229:13–23.
16. Helisch A, Schaper W (2003) *Microcirculation* 10:83–97.
17. Ramesh R, Mhashilkar AM, Tanaka F, Saito Y, Branch CD, Sieger K, Mumm JB, Stewart AL, Boquoi A, Dumoutier L, *et al.* (2003) *Cancer Res* 63:5105–5113.
18. Liu Z-J, Xiao M, Balint K, Soma A, Pinnix CC, Capobianco AJ, Velazquez OC, Herlyn M (2006) *FASEB J* 20:E201–E210.
19. Krebs LT, Xue Y, Norton CR, Shutter JR, Maguire M, Sundberg JP, Gallaha D, Closson V, Kitajewski J, Callahan R, *et al.* (2000) *Genes Dev* 14:1343–1352.
20. Pugh CW, Ratcliffe PJ (2003) *Nat Med* 9:677–684.
21. Simons M (2005) *Circulation* 111:1556–1566.
22. Henry TD, Annex BH, McKendall GR, Azrin MA, Lopez JJ, Giordano FJ, Shah PK, Willerson JT, Benza RL, Berman DS, *et al.* (2003) *Circulation* 107:1359–1365.
23. Cao Y, Linden P, Farnebo J, Cao R, Eriksson A, Kumar V, Qi JH, Claesson-Welsh L, Alitalo K (1998) *Proc Natl Acad Sci USA* 95:14389–14394.
24. Eriksson A, Cao R, Roy J, Tritsaris K, Wahlestedt C, Dissing S, Thyberg J, Cao Y (2003) *Circulation* 107:1532–1538.
25. Dissing S, Nauntofte B, Sten-Knudsen O (1990) *Eur J Physiol* 417:1–12.
26. Korff T, Augustin HG (1999) *J Cell Sci* 112:3249–3258.
27. Cao Y, Cao R (1999) *Nature* 398:381.